Report
P-21-06
April 2021

Modelling of the long term diffusion and sorption experiment using an analytically solvable model

Task 9 of SKB Task Force GWFTS – Increasing the realism in solute transport modelling based on the field experiments REPRO and LTDE-SD

Pekka Kekäläinen

SVENSK KÄRNBRÄNSLEHANTERING AB

SWEDISH NUCLEAR FUEL
AND WASTE MANAGEMENT CO

Box 3091, SE-169 03 Solna
Phone +46 8 459 84 00
skb.se

SVENSK KÄRNBRÄNSLEHANTERING

ISSN 1651-4416
SKB P-21-06
ID 1930249

April 2021

Modelling of the long term diffusion and sorption experiment using an analytically solvable model

Task 9 of SKB Task Force GWFTS – Increasing the realism in solute transport modelling based on the field experiments REPRO and LTDE-SD

Pekka Kekäläinen, University of Helsinki

Keywords: Modelling, Diffusion, Sorption, Tracers, Rock matrix.

Abstract

We study modelling of the Long Term Diffusion and Sorption Experiment using analytically solvable sorption-diffusion models for activity profiles of the sample cores and the time evolution of the tracer concentration in the aqueous phase.

The model was fitted to the measured activity profiles of the sample cores. From the optimal values of the fitting parameters we calculated the linear equilibrium sorption constant K_d for the tracers. The results were nicely compatible with laboratory measurements. The evolution of tracer concentrations in the solution reservoir was modelled separately. Good matches were obtained for ^{133}Ba, ^{137}Cs, ^{109}Cd and ^{226}Ra.

Sammanfattning

Modellering av Long Term Diffusion and Sorption Experiment med användning av analytiskt lösbara sorptions- och diffusionsmodeller för aktivitetsprofiler i provkärnor samt förändringen över tid med avseende på koncentrationen av radionuklider i vattenfasen har studerats.

Modellen anpassades till de uppmätta aktivitetsprofilerna för provkärnorna. Från de optimala värdena för anpassningsparametrarna beräknade vi den linjära jämviktssorptionskonstanten K_d för radionukliderna. Resultaten var kompatibla med laboratoriemätningar. Förändringen av spårämneskoncentrationerna i injektionsområdet modellerades separat. Bra överenstämmelser uppnåddes för ^{133}Ba, ^{137}Cs, ^{109}Cd och ^{226}Ra.

Contents

1 Introduction 7

2 The mathematical model 9
2.1 Homogeneous rock matrix 9
2.1.1 A-cores 9
2.1.2 D-cores 10
2.1.3 Fitting to the measured data 10
2.2 Rock matrix with two components 11
2.2.1 Fitting to the measured data 11
2.3 Aqueous phase 12

3 Results 15
3.1 Penetration profiles 15
3.2 Rock matrix vs. aqueous phase in the solution reservoir 15

4 Summary and conclusions 17

References 19

Appendix A The solution of the model for A-cores 21

Appendix B The solution of the model for D-cores 23

Appendix C The solution of the aqueous phase model 25

Appendix D The optimal values of the fitting parameters 27

Appendix E Fitting figures for the penetration profiles 29

Appendix F Plots of the aqueous phase model 43

1 Introduction

In this report we consider mathematical modelling of the Long Term Diffusion and Sorption Experiment (LTDE-SD) performed in the SKB Äspö Hard Rock Laboratory. A description of LTDE-SD can be found in Widestrand et al. (2010). Our aim is to study how well the experimental results can be modelled with a simple sorption-diffusion model. This work is a contribution to Task 9B (Löfgren and Nilsson 2020) performed in the SKB Task Force GWFTS.

In the first case we consider Fickian diffusion in a homogeneous rock matrix with linear adsorption isotherm and an instantaneous equilibrium between solid and liquid phases. For the spatial distribution of the tracer in the core we get an expression with two fitting parameters, the apparent diffusion coefficient D_a and

$$K = \frac{\epsilon + (1-\epsilon)\, K_d\, \rho_{rock}}{\epsilon\, \rho_{water} + (1-\epsilon)\rho_{rock}},$$

where ϵ is the porosity of the rock and K_d is a linear equilibrium sorption constant. Using these parameters as fitting parameters we fit our model to the measured penetration curves of tracers.

Inhomogeneity of the rock is included into our model by considering two independent parallel sorption-diffusion processes in two different materials. In this way we get (an analytically solvable) model with four parameters: a similar K as above, where K_d is the linear equilibrium sorption constant of the composition, apparent diffusion coefficients of different materials and a parameter which is related to the fractions of different materials and their retention capacities.

In the homogeneous case we construct a simple (analytically solvable) model for the time evolution of the concentration of the tracer in the aqueous phase.

2 The mathematical model

In following we construct a mathematical model for the measured concentration profiles, which takes into account the diffusion and the sorption in the rock matrix during the in situ and the storing periods of the experiment.

2.1 Homogeneous rock matrix

Assume that the tracer is only transported by diffusion in the water phase of the rock matrix. The concentration of the tracer in the water phase C (mass of tracer/volume of water) and sorbed on the rock matrix C_s (mass of sorbed tracer/mass of rock) can be described with the equation

$$\epsilon \frac{\partial C}{\partial t} + (1-\epsilon)\,\rho_r \frac{\partial C_s}{\partial t} - \nabla \cdot (\epsilon\, D_p \nabla C) = 0, \tag{2-1}$$

where ϵ is the porosity, ρ_r the density of the rock and D_p is the pore diffusion coefficient of the tracer in the porous matrix. During the in situ period of the experiment the boundary condition on the surface of the rock is

$$C(\mathbf{x},t) = C_0(t), \tag{2-2}$$

where $C_0(t)$ is the measured concentration of the tracer in the aqueous phase and $\mathbf{x}$ lies on the surface between the rock and the aqueous phase. During the storing period there is no flux of the tracer through the surface of the rock. So in this period we get boundary conditions

$$\mathbf{n} \cdot \nabla C(\mathbf{x},t) = 0,\ \mathbf{n} \cdot \nabla C_s(\mathbf{x},t) = 0, \tag{2-3}$$

where $\mathbf{n}$ is a unit normal of the boundary surface. Assume that the rock matrix is homogeneous and the sorption is governed by a linear equilibrium isotherm and an instantaneous equilibrium between solid and liquid phases. So

$$K_d = \frac{C_s}{C} \tag{2-4}$$

where K_d is a linear equilibrium sorption constant and the Equation (2-1) leads to a diffusion equation

$$\frac{\partial C}{\partial t} - D_a \Delta C = 0 \tag{2-5}$$

where D_a is the apparent diffusion coefficient

$$D_a = \frac{\epsilon\, D_p}{\epsilon + (1-\epsilon)\,\rho_r\, K_d}. \tag{2-6}$$

2.1.1 A-cores

In the test section stub (A-cores) we may assume that diffusion is one dimensional. In this case the system can be described with a one dimensional diffusion equation

$$\frac{\partial C}{\partial t} - D_a \frac{\partial^2 C}{\partial x^2} = 0, \tag{2-7}$$

with the boundary condition

$$C(0,t) = C_0(t),\ \ 0 \le t \le t_0,$$

$$\frac{\partial C}{\partial x}(0,t) = 0,\ \ t > t_0, \tag{2-8}$$

where $C_0(t)$ is the measured aqueous concentration and t_0 is the duration of the in situ period of the experiment. At the other end of core sample $x = L$ we can use the boundary condition

$$\frac{\partial C}{\partial x}(L,t) = 0\,. \tag{2-9}$$

The initial condition is

$$C(x,0) = 0. \tag{2-10}$$

At the beginning of the experiment the measured aqueous concentration $C_0(t)$ decreased quite fast and after that it did not vary much. So, for simplicity we can assume, that $C_0(t) = C_0$ is a constant. Now the solution our problem can be written in the form

$$C(x,t) = C_0\,(u(\tfrac{x}{L}, \tfrac{D_a t}{L^2}; \tfrac{D_a t_0}{L^2}) + 1), \tag{2-11}$$

where an expression for function u is derived in the Appendix A.

2.1.2 D-cores

In the test section slim-hole (D-cores) we describe the system with a radial diffusion equation (in the cylindrical coordinates)

$$\frac{\partial C}{\partial t} - D_a\left(\frac{\partial^2 C}{\partial r^2} + \frac{1}{r}\frac{\partial C}{\partial r}\right) = 0, \tag{2-12}$$

with similar boundary conditions as above

$$\begin{aligned} &C(a,t) = C_0(t), \quad 0 \le t \le t_0, \\ &\frac{\partial C}{\partial r}(a,t) = 0\,, \quad t > t_0, \\ &\frac{\partial C}{\partial r}(R,t) = 0\,, \end{aligned} \tag{2-13}$$

where a is the radius of the drill hole and R is the radius of the over-cored cylinder. For the constant boundary condition $C_0(t) = C_0$ and zero initial condition

$$C(r,0) = 0 \tag{2-14}$$

we can solve the problem analytically. The solution can be written in the form

$$C(r,t) = C_0\,(v(\tfrac{r}{a}, \tfrac{D_a t}{a^2}; \tfrac{D_a t_0}{a^2}) + 1), \tag{2-15}$$

where an expression for function v is derived in the Appendix B.

2.1.3 Fitting to the measured data

The measured data is the tracer activity concentration [Bq/g] in the slices from cores, i.e.

$$A = \frac{A_{tr}\, m}{M}, \tag{2-16}$$

where A_{tr} is the activity of the tracer [Bq/g], m the mass of the tracer in the slice and M is the mass of the slice. The data gives us the spatial distribution of the activity in a core at the time $t = t_0 + t_1$, where t_0 is the duration of the in situ period of the experiment and t_1 is the time from the end of the in situ experiment to the slicing of the core. The spatial distribution of the activity in an A-core (at the time $t = t_0 + t_1$) predicted with our model is given by

$$A(x) = K A_0\,(u(\tfrac{x}{L}, \tfrac{D_a (t_0 + t_1)}{L^2}; \tfrac{D_a t_0}{L^2}) + 1), \tag{2-17}$$

and for D-cores

$$A(r) = K A_0\,(v(\tfrac{r}{a}, \tfrac{D_a (t_0 + t_1)}{a^2}; \tfrac{D_a t_0}{a^2}) + 1). \tag{2-18}$$

Here $A_0 = C_0 A_{tr}$ is the measured activity of the aqueous phase and

$$K = \frac{\epsilon + (1-\epsilon) K_d \rho_r}{\epsilon \rho_w + (1-\epsilon)\rho_r}, \tag{2-19}$$

and ρ_w is the density of water. Now we can fit our model to the measured data using K and D_a as fitting parameters.

2.2 Rock matrix with two components

A simple model for diffusion in a rock matrix consisting of two different materials (porosities ϵ_i and densities ρ_i, $i = 1, 2$) can be described with two independent sorption-diffusion processes

$$\epsilon_i \frac{\partial C_i}{\partial t} + (1-\epsilon_i)\rho_i \frac{\partial C_{si}}{\partial t} - \nabla \cdot \left(\epsilon_i D_p^{(i)} \nabla C_i\right) = 0\,, \quad (i = 1\,,\ 2), \tag{2-20}$$

with the same boundary conditions (2-2) and (2-3) for both components. Using similar assumptions as before ($K_d^{(i)} = C_{si}/C_i$), we can describe our system with two diffusion equations

$$\frac{\partial C_i}{\partial t} - D_a^{(i)} \Delta C_i = 0, \tag{2-21}$$

where

$$D_a^{(i)} = \frac{\epsilon_i D_p^{(i)}}{\epsilon_i + (1-\epsilon_i)\rho_i K_d^{(i)}}\,. \tag{2-22}$$

For A-cores Equations (2-21) reduce to one dimensional diffusion equations, and for D-cores to radial diffusion equations. With the similar initial and boundary conditions we can solve these equations in the same way as in the homogeneous case, and the solution for A-cores (resp. D-cores) is

$$C_i(x,t) = C_0\, u_i(x,t), \text{ (resp. } C_i(r,t) = C_0\, v_i(r,t)), \tag{2-23}$$

where

$$u_i(\mathrm{x},\mathrm{t}) = u(\tfrac{x}{L}, \tfrac{D_a^{(i)} t}{L^2}; \tfrac{D_a^{(i)} t_0}{L^2}) + 1\,, \tag{2-24}$$
$$v_i(\mathrm{r},\mathrm{t}) = v(\tfrac{r}{a}, \tfrac{D_a^{(i)} \mathrm{t}}{a^2}; \tfrac{D_a^{(i)} t_0}{a^2}) + 1\,.$$

2.2.1 Fitting to the measured data

Consider first A-cores. In this case the activity profile in the component i (at the time $t = t_0 + t_1$) is given by

$$A_i(x) = K_i\ A_0\, u_i(x, t_0 + t_1), \tag{2-25}$$

where $A_0 = A_{tr} C_0$ is the activity of the aqueous phase and

$$K_i = \frac{\epsilon_i + (1-\epsilon_i) K_d^{(i)} \rho_i}{\epsilon_i \rho_w + (1-\epsilon_i)\rho_i}. \tag{2-26}$$

The spatial distribution of the activity in the composition with the volume fraction p of the component 1 and $q = 1-p$ of the component 2 is

$$A(x) = p_1 A_1(x) + p_2 A_2(x) \tag{2-27}$$

where

$$p_1 = \frac{p(1-\epsilon_1)\rho_1 + p\,\epsilon_1 \rho_w}{p(1-\epsilon_1)\rho_1 + q(1-\epsilon_2)\rho_2 + (p\,\epsilon_1 + q\,\epsilon_2)\rho_w}\,, \tag{2-28}$$
$$p_2 = \frac{q(1-\epsilon_2)\rho_2 + q\,\epsilon_2\,\rho_w}{p(1-\epsilon_1)\rho_1 + q(1-\epsilon_2)\rho_2 + (p\,\epsilon_1 + q\,\epsilon_2)\rho_w}\,.$$

The distribution coefficient K_d the composition is

$$K_d = \frac{p(1-\epsilon_1)\rho_1 K_d^{(1)} + q(1-\epsilon_2)\rho_2 K_d^{(2)}}{p(1-\epsilon_1)\rho_1 + q(1-\epsilon_2)\rho_2}. \tag{2-29}$$

Since

$$p_1 K_1 + p_2 K_2 = \frac{\epsilon + (1-\epsilon) K_d \rho_r}{\epsilon \rho_w + (1-\epsilon)\rho_r} =: K, \tag{2-30}$$

where ϵ and ρ_r are the average porosity and density of the rock

$$\epsilon = p\epsilon_1 + q\epsilon_2, \tag{2-31}$$

$$\rho_r = \frac{p(1-\epsilon_1)\rho_1 + q(1-\epsilon_2)\rho_2}{p(1-\epsilon_1) + q(1-\epsilon_2)},$$

we can write the formula (2-27) in the form

$$A(x) = K A_0 (\alpha u_1(x, t_0 + t_1) + (1-\alpha) u_2(x, t_0 + t_1)), \tag{2-32}$$

where

$$\alpha = \frac{p_1 K_1}{p_1 K_1 + p_2 K_2}. \tag{2-33}$$

Now we can fit (2-32) to the measured data using K, $D_a^{(1)}$, $D_a^{(2)}$ and α as fitting parameters.

For D-cores we can proceed in the same way, and we can write the spatial distribution of the activity of the composition in a similar form

$$A(r) = K A_0 (\alpha v_1(x, t_0 + t_1) + (1-\alpha) v_2(x, t_0 + t_1)), \tag{2-34}$$

with the same parameters K and α as above.

2.3 Aqueous phase

Let the concentration of the tracer in the rock matrix be described by the Equations (2-1) and (2-2). Assume that the aqueous phase is well mixed. Then the concentration of the tracer in the aqueous phase $C_0(t)$ is driven by the equation

$$V \frac{dC_0}{dt} + \int_A \frac{\partial S}{\partial t}\, dA = \int_A \epsilon D_p \nabla C \cdot d\bar{A}. \tag{2-35}$$

Here V is the volume of the aqueous phase, and S is the concentration of the tracer on the surface of the rock and the right hand side of the equation is the flux of the tracer into the rock matrix. We assume that sorption on the surface of the rock happens immediately, and the concentration S remains constant after that. Under these assumptions we can eliminate the integral term on the left hand side of the equation by rescaling the initial value $C_0(0)$. With similar assumptions as in the case of homogeneous rock our system can be described by equations:

$$
\begin{aligned}
&\frac{\partial C_1}{\partial t} - D_a \frac{\partial^2 C_1}{\partial x^2} = 0, \quad 0 < x < L,\\
&\frac{\partial C_2}{\partial t} - \left(\frac{\partial^2 C_2}{\partial r^2} + \frac{1}{r} \frac{\partial C_2}{\partial r} \right) = 0, \; a < r < R,\\
&C_1(L,t) = 0, \; C_2(R,t) = 0,\\
&C_0(t) = C_1(0,t) = C_2(a,t),\\
&V \frac{dC_0}{dt} = \epsilon A_1 D_p \frac{\partial C_1}{\partial x}(0,t) + \epsilon A_2 D_p \frac{\partial C_2}{\partial r}(a,t),\\
&C_1(x,0) = \begin{cases} C_0, & x = 0 \\ 0, & x > 0, \end{cases} \qquad C_2(r,0) = \begin{cases} C_0, & r = a \\ 0, & r > a. \end{cases}
\end{aligned}
\tag{2-36}
$$

Here C_1 (resp. C_2) is the concentration of the tracer in the water phase of the rock in the test section stub (resp. test section slim-hole), A_1 (resp. A_2) is the area of the surface between aqueous phase and the rock matrix in the test section stub (resp. test section slim-hole), and the constant C_0 is the rescaled initial concentration of the tracer in the aqueous phase. The solution of this system is constructed in the Appendix C.

3 Results

3.1 Penetration profiles

For ^{133}Ba, ^{57}Co, ^{109}Cd, ^{63}Ni and ^{226}Ra there were only few data points, and the beginning of penetration curves were nicely fitted with homogeneous model. Deeper in cores there is "background", which can be taken into account by adding a constant to the model. We have not considered physical nor experimental grounds of this background. Optimal values of the fitting parameters are listed in the Table D-1. We used D_a and K (see (2-19)) and as fitting parameters, K_d is calculated using the values $\epsilon = 0.3$ % and $\rho_r = 2\,700$ kg/m^3 for the porosity and the density of the rock (Nilsson et al. 2010). For the concentration C_0 in the aqueous phase we have used the values listed in the Table 3-1. These values are the average concentration in the reservoir in the period $70d$–$189d$ ($133d$–$189d$ for ^{63}Ni and ^{109}Cd since their concentration was clearly decreasing after $70d$).

Table 3-1: The values of the concentration C_0 [Bq/ml] in the aqueous phase used in the fittings.

^{133}Ba	^{63}Ni	^{57}Co	^{226}Ra	^{109}Cd	^{137}Cs	^{22}Na	^{36}Cl
1050	8600	120	58	4400	2900	2830	5130

For ^{137}Cs we used also the two-component model for some of the cores. The effect of the second component appeared at very low concentrations, i.e. the parameter α was very close to one. For ^{22}Na the homogeneous model worked only with two cores. In several cores the concentration profile of ^{22}Na was not decreasing near the surface between the rock and the aqueous phase. Possible reason for this is the heterogeneity of the rock, i.e. the average K_d is not the same in different slides. Since ^{22}Na is quite weakly sorbing also a part of the tracer might have flushed away during the slicing of cores.

For ^{133}Ba, ^{57}Co, ^{226}Ra, ^{109}Cd and ^{137}Cs the (average) values for K_d obtained from our fittings are nicely compatible with the values obtained in laboratory measurements. For ^{63}Ni and ^{22}Na our optimal values were about one order of magnitude smaller than values from laboratory measurements (Nilsson et al. 2010).

We treated ^{36}Cl as a non sorbing tracer, and instead of K_d we used the porosity ϵ as a fitting parameter.

Optimal values of the fitting parameters are listed in the Tables in the Appendix D and all of the fitted plots are presented in the Appendix E. Red (resp. blue) curves correspond to 240 (resp. 290) days storing period.

3.2 Rock matrix vs. aqueous phase in the solution reservoir

The measured concentrations of ^{133}Ba and ^{137}Cs in the aqueous phase and plots of the constructed model are shown in the Figure F-1 in Appendix F. In the fitted curves average values from the penetration fits has been used: $D_a = 4.4 \times 10^{-14}$ m^2/s and $K_d = 1.5 \times 10^{-3}$ m^3/kg for ^{133}Ba and $D_a = 4.3 \times 10^{-14}$ m^2/s and $K_d = 9.0 \times 10^{-3}$ m^3/kg for ^{137}Cs. Our model fits also nicely to the data of ^{109}Cd and ^{226}Ra (Figure F-2 in Appendix F), but with slightly different values of parameters than the averages from the penetration fittings ($D_a = 5 \times 10^{-14}\, m^2/s$ and $K_d = 6 \times 10^{-3}$ m^3/kg for ^{109}Cd and $D_a = 2 \times 10^{-14}$ m^2/s and $K_d = 5 \times 10^{-3}$ m^3/kg for ^{226}Ra). For ^{63}Ni we got a nice fit with parameters $D_a = 1.8 \times 10^{-14}$ m^2/s and $K_d = 1.5 \times 10^{-2}$ m^3/kg; the value of K_d is about one order of magnitude larger than the optimal value obtained from the fittings of penetration curves. For these tracers there were penetration data only from few cores, so the overall average of D_a and K_d might be different than the average of the existing data. The modelling of the aqueous phase was not performed for ^{22}Na and ^{36}Cl due to large oscillations in the measured data. The measured data of ^{57}Co did not fit to our model at all (Figure F-3 in Appendix F).

4 Summary and conclusions

Our idea was to construct a sorption-diffusion model for activity profiles of the cores, which takes into account different boundary conditions during the in situ and the storing periods of the experiment. Because there were only few measured data points in activity profiles of strongly sorbing tracers, we made our model as simple as possible. We considered Fickian diffusion in a homogeneous rock matrix with linear adsorption isotherm and an instantaneous equilibrium between solid and liquid phases. In this case we had two independent parameters in our model. This two-parameter model did not give the correct shape for the penetration curves of ^{22}Na and ^{36}Cl. So, we constructed a two-component model by considering two independent parallel sorption-diffusion processes in two different materials. In the homogeneous case we constructed a model for the time evolution of the concentration of the tracer in the aqueous phase. Our models can be solved analytically in the terms of series expressions. The solutions look a little bit complicated but they are useful for numerical calculations: the eigenvalues appearing in the expressions can be easily computed numerically and the series expressions are quite rapidly converging.

For strongly sorbing tracers there were only few data points, and the beginning of penetration curves were nicely fitted with homogeneous model, but deeper in cores there is “background”. We have not considered physical or experimental grounds of this background in detail. This background is possibly caused by contamination during sample preparation, and we took it into account by adding a constant to the model. The values of the linear sorption constant K_d obtained from the fittings of penetration curves were nicely compatible with values from batch sorption laboratory measurements for matrix rock for ^{133}Ba, ^{57}Co, ^{226}Ra, ^{109}Cd and ^{137}Cs. For ^{63}Ni and ^{22}Na the optimal values of K_d were about one order of magnitude smaller than values from laboratory measurements.

The measured concentrations of tracers in the aqueous phase, and plots of the constructed model with the parameters obtained from the fittings of penetration curves, were nicely compatible for strongly sorbing tracers except for ^{63}Ni and ^{57}Co. Our model also worked for ^{63}Ni with an order magnitude larger K_d. The time evolution of the concentration of ^{57}Co in the aqueous phase was not monotonically decreasing, so it could not be modelled with a pure diffusion process, but chemistry must also be included.

References

SKB's (Svensk Kärnbränslehantering AB) publications can be found at www.skb.com/publications.

Löfgren M, Nilsson K, 2020. Task description of Task 9B – Modelling of LTDE-SD performed at Äspö HRL. Task 9 of SKB Task Force GWFTS – Increasing the realism in solute transport modelling based on the field experiments REPRO and LTDE-SD. SKB P-17-30, Svensk Kärnbränslehantering AB.

Nilsson K, Byegård B, Selnert E, Widestrand H, Höglund S, Gustafsson E, 2010. Äspö Hard Rock Laboratory. Long Term Sorption Diffusion Experiment (LTDE-SD). Results from rock sample analyses and modelling, SKB R-10-68, Svensk Kärnbränslehantering AB.

Widestrand H, Byegård J, Nilsson K, Höglund S, Gustafsson E, Kronberg M, 2010. Long Term Sorption Diffusion Experiment (LTDE-SD). Performance of main in situ experiment and results from water phase measurements. SKB R-10-67, Svensk Kärnbränslehantering AB.

Appendix A

The solution of the model for A-cores

With the substitution

$$\xi = \frac{x}{L},\ \tau = \frac{D_a t}{L^2},\ C(x,t) = C_0(u(\xi,\tau;\tau_0)+1) \tag{A-1}$$

we can write the problem (2-5)–(2-10) in a dimensionless form

$$\frac{\partial u}{\partial \tau} - \frac{\partial^2 u}{\partial \xi^2} = 0,$$

$$\begin{cases} u(0,\tau) = 0,\ 0 \le \tau \le \tau_0, \\ \dfrac{\partial u}{\partial \xi}(0,\tau) = 0,\ \tau > \tau_0, \end{cases} \tag{A-2}$$

$$\frac{\partial u}{\partial \xi}(1,\tau) = 0,$$

$$u(\xi, 0) = -1,$$

where $\tau_0 = \frac{D_a t_0}{L^2}$. The Equation (A-2) can be solved by separating the variables. In the time interval $0 \le \tau \le \tau_0$ the solution can be written in the form

$$u(\xi,\tau;\tau_0) = -2\sum_{n=0}^{\infty} \frac{e^{-\mu_n^2 \tau}}{\mu_n} \sin \mu_n \xi, \tag{A-3}$$

where $\mu_n = (n + \frac{1}{2})\pi$. For $\tau > \tau_0$ the function u is the solution of the

boundary value problem

$$\frac{\partial u}{\partial \tau} - \frac{\partial^2 u}{\partial \xi^2} = 0, \tag{A-4}$$

$$\frac{\partial u}{\partial \xi}(0,\tau) = \frac{\partial u}{\partial \xi}(1,\tau) = 0,$$

with the initial condition

$$u(\xi, \tau_0) = -2\sum_{n=0}^{\infty} \frac{e^{-\mu_n^2 \tau_0}}{\mu_n} \sin \mu_n \xi. \tag{A-5}$$

We can solve this equation by separating the variables, and the solution can be written as a series expression

$$u(\xi,\tau;\tau_0) = a_0 + \sum_{n=1}^{\infty} a_n e^{-\lambda_n^2(\tau-\tau_0)} \cos \lambda_n \xi,\ (\tau \ge \tau_0) \tag{A-6}$$

where $\lambda_n = n\pi$ and

$$a_0 = -2\sum_{m=0}^{\infty} \frac{e^{-\mu_m^2 \tau_0}}{\mu_m^2},\ a_n = -4\sum_{m=0}^{\infty} \frac{e^{-\mu_m^2 \tau_0}}{\mu_m^2 - \lambda_n^2}. \tag{A-7}$$

Appendix B

The solution of the model for D-cores

We can proceed in the same way as above, with the substitution

$$\rho = \frac{r}{a},\ \tau = \frac{D_a t}{a^2},\ \ C(r,t) = C_0(v(\rho,\tau;\tau_0)+1) \tag{B-1}$$

we can write the problem (2-12)–(2-14) in a dimensionless form

$$\frac{\partial v}{\partial \tau} - \left(\frac{\partial^2 v}{\partial \rho^2} + \frac{1}{\rho}\frac{\partial v}{\partial \rho}\right) = 0,$$

$$\begin{cases} v(1,\tau) = 0, & 0 \le \tau \le \tau_0, \\ \dfrac{\partial v}{\partial \rho}(1,\tau) = 0, & \tau > \tau_0, \end{cases} \tag{B-2}$$

$$\frac{\partial v}{\partial \rho}(\rho_0,\tau) = 0,$$

$$v(\rho,0) = -1,$$

where $\tau_0 = \frac{D_a t_0}{a^2}$ and $\rho_0 = R/a$. Separation of the variables leads to a Bessel

equation for the radial part ϕ

$$\frac{d^2\phi}{d\rho^2} + \frac{1}{\rho}\frac{d\phi}{d\rho} + \mu^2\phi = 0. \tag{B-3}$$

In the time interval $0 \le \tau \le \tau_0$ we get boundary conditions

$$\phi(1) = 0, \quad \frac{d\phi}{d\rho}(\rho_0) = 0. \tag{B-4}$$

Eigenfunctions ϕ_n satisfying the eigenvalue problem (B-3)–(B-4) can be written as a combination of Bessel functions J_0 and Y_0 in the form

$$\phi_n(\rho) = Y_0(\mu_n)J_0(\mu_n\rho) - J_0(\mu_n)Y_0(\mu_n\rho), \tag{B-5}$$

where the eigenvalues $0 < \mu_1 < \mu_2 < \cdots$ are the roots of the equation

$$Y_0(\mu)J_1(\mu\rho_0) - J_0(\mu)Y_1(\mu\rho_0) = 0. \tag{B-6}$$

In the time interval $0 \le \tau \le \tau_0$ the solution can be written in the form

$$v(\rho,\tau;\tau_0) = \pi \sum_{n=1}^{\infty} \frac{e^{-\mu_n^2 \tau} J_1(\mu_n\rho_0)^2}{J_0(\mu_n)^2 - J_1(\mu_n\rho_0)^2}\,\phi_n(\rho). \tag{B-7}$$

For $\tau > \tau_0$ the function v is the solution of the boundary value problem

$$\frac{\partial v}{\partial \tau} - \left(\frac{\partial^2 v}{\partial \rho^2} + \frac{1}{\rho}\frac{\partial v}{\partial \rho}\right) = 0, \tag{B-8}$$

$$\frac{\partial v}{\partial \rho}(1,\tau) = 0, \quad \frac{\partial v}{\partial \rho}(\rho_0,\tau) = 0,$$

with the initial condition (at $\tau = \tau_0$)

$$v(\rho,\tau_0;\tau_0) = \pi \sum_{n=1}^{\infty} \frac{\mathrm{e}^{-\mu_n^2 \tau_0} J_1(\mu_n\rho_0)^2}{J_0(\mu_n)^2 - J_1(\mu_n\rho_0)^2}\,\phi_n(\rho). \tag{B-9}$$

In this case the separation of the variables leads to a Bessel equation for the radial part ψ

$$\frac{d^2\psi}{d\rho^2} + \frac{1}{\rho}\frac{d\psi}{d\rho} + \lambda^2\,\psi = 0, \tag{B-10}$$

with the boundary conditions

$$\frac{d\psi}{d\rho}(1) = 0, \quad \frac{d\psi}{d\rho}(\rho_0) = 0 \tag{B-11}$$

In this case the eigenvalues are $\lambda_0 = 0$ and $0 < \lambda_1 < \lambda_2 < \cdots$ are the roots of the equation

$$Y_1(\lambda)J_1(\lambda\rho_0) - J_1(\lambda)\,Y_1(\lambda\rho_0) = 0, \tag{B-12}$$

and corresponding eigenfunctions are $\psi_0 = 1$ and

$$\psi_n(\rho) = Y_1(\lambda_n)J_0(\lambda_n\rho) - J_1(\lambda_n)\,Y_0(\lambda_n\rho). \tag{B-13}$$

For $\tau \geq \tau_0$ the solution of the problem (B-2) can be written as a series expression

$$v(\rho, \tau\,; \tau_0) = a_0 + \sum_{n=1}^{\infty} a_n\, e^{-\lambda_n^2(\tau - \tau_0)}\,\psi_n(\rho), \tag{B-14}$$

where the coefficients a_n are

$$a_0 = -\frac{4}{\rho_0^2 - 1}\sum_{m=1}^{\infty}\frac{e^{-\mu_m^2\,\tau_0}\,J_1(\mu_m\rho_0)^2}{\mu_m^2\,(J_0(\mu_m)^2 - J_1(\mu_m\rho_0)^2)} \tag{B-15}$$

and

$$a_n = \frac{2\,\pi\lambda_n\,J_1(\lambda_n\rho_0)^2}{J_1(\lambda_n)^2 - J_1(\lambda_n\rho_0)^2}\sum_{m=1}^{\infty}\frac{e^{-\mu_m^2\,\tau_0}\,J_1(\mu_m\rho_0)^2}{(\mu_m^2 - \lambda_n^2)(J_0(\mu_m)^2 - J_1(\mu_m\rho_0)^2)} \tag{B-16}$$

Appendix C

The solution of the aqueous phase model

With the substitution

$$\xi = \frac{x}{L}, \quad \rho = \frac{r}{a}, \quad \tau = \frac{D_a t}{a^2}, \tag{C-1}$$

$$C_1(x,t) = C_0\, u_1(\xi,\tau),\ \ C_2(r,t) = C_0\, u_2(\rho,\tau)$$

we can write the Equation (2-36) in a dimensionless setting:

$$\begin{aligned}
&\frac{\partial u_1}{\partial \tau} - \mu^2 \frac{\partial^2 u_1}{\partial \xi^2} = 0,\ \ 0 < \xi < 1,\\
&\frac{\partial u_2}{\partial \tau} - \left(\frac{\partial^2 u_2}{\partial \rho^2} + \frac{1}{r}\frac{\partial u_2}{\partial \rho} \right) = 0,\ \ 1 < \rho < \rho_0,\\
&u_1(1,\tau) = 0,\ \ u_2(\rho_0,\tau) = 0, \qquad \text{(C-2)}\\
&u_1(0,\tau) = u_2(1,\tau),\\
&\frac{\partial u_1}{\partial \tau}(0,\tau) = \alpha \frac{\partial u_1}{\partial \xi}(0,\tau) + \beta \frac{\partial u_2}{\partial \rho}(1,\tau),\\
&u_1(\xi,0) = \begin{cases} 1, & \xi = 0 \\ 0, & 0 < \xi \le 1, \end{cases} \qquad u_2(\rho,0) = \begin{cases} 1, & \rho = 1 \\ 0, & 1 < \rho \le \rho_0, \end{cases}
\end{aligned}$$

where the dimensionless parameters are

$$\begin{aligned}
&\mu = \frac{a}{L},\ \ \rho_0 = \frac{R}{a},\\
&\alpha = (\epsilon + (1-\epsilon) K_d \rho_r) \frac{A_1 a^2}{L V}, \qquad \text{(C-3)}\\
&\beta = (\epsilon + (1-\epsilon) K_d \rho_r) \frac{A_2 a}{V}.
\end{aligned}$$

The solution of the Equation (C-2) can be constructed by separating the variables. The separation

$$u_1(\xi,\tau) = w(\tau) v_1(\xi), \quad u_2(\rho,\tau) = w(\tau) v_2(\rho) \tag{C-4}$$

leads to differential equations

$$\frac{d^2 v_1}{d\xi^2} + \left(\frac{\lambda}{\mu}\right)^2 v_1 = 0, \quad \frac{d^2 v_2}{d\rho^2} + \frac{1}{\rho}\frac{dv_2}{d\rho} + \lambda^2 v_2 = 0, \tag{C-5}$$

with eigenvalue dependent boundary conditions

$$\begin{aligned}
&v_1(1) = 0, \ \ v_2(\rho_0) = 0, \ \ v_1(0) = v_2(1), \qquad \text{(C-6)}\\
&-\lambda^2 v_1(0) = \alpha \frac{dv_1}{d\xi}(0) + \beta \frac{dv_2}{d\rho}(1).
\end{aligned}$$

Solutions of the boundary value problem (C-5)–(C-6) are

$$\begin{aligned}
&v_1^{(n)}(\xi) = \left(Y_0(\lambda_n \rho_0) J_0(\lambda_n) - J_0(\lambda_n \rho_0) Y_0(\lambda_n) \right) \sin \frac{\lambda_n}{\mu}(1-\xi), \qquad \text{(C-7)}\\
&v_2^{(n)}(\rho) = \sin \frac{\lambda_n}{\mu} \left(Y_0(\lambda_n \rho_0) J_0(\lambda_n \rho) - J_0(\lambda_n \rho_0) Y_0(\lambda_n \rho) \right),
\end{aligned}$$

where the eigenvalues $0 < \lambda_1 < \lambda_2 < \cdots$ are the positive roots of the equation

$$J_0(\lambda\rho_0)\left\{\beta \sin\frac{\lambda}{\mu}\, Y_1(\lambda) - \left(\lambda \sin\frac{\lambda}{\mu} - \frac{\alpha}{\mu}\cos\frac{\lambda}{\mu}\right) Y_0(\lambda)\right\} \tag{C-8}$$
$$= Y_0(\lambda\rho_0)\left\{\beta \sin\frac{\lambda}{\mu} J_1(\lambda) - \left(\lambda \sin\frac{\lambda}{\mu} - \frac{\alpha}{\mu}\cos\frac{\lambda}{\mu}\right) J_0(\lambda)\right\}$$

The (pairs of the) functions $(v_1^{(n)}, v_2^{(n)})$ are orthogonal with respect to the inner product

$$\langle (v_1, v_2) \mid (u_1, u_2)\rangle$$
$$= \frac{\alpha}{\mu^2}\int_0^1 v_1(\xi)\, u_1(\xi)\, d\xi + \beta\int_1^{\rho_0} v_2(\rho)\, u_2(\rho)\, \rho\, d\rho \tag{C-9}$$
$$+\frac{1}{2}(v_1(0)\, u_1(0) + v_2(1)\, u_2(1)).$$

Now the solution of the problem (C-2) can be written as a series expression

$$(u_1(\xi, \tau), u_2(\rho, \tau)) = \sum_{n=1}^{\infty} \frac{a_n\, e^{-\lambda_n^2}}{b_n}\,(v_1^{(n)}(\xi), v_2^{(n)}(\rho)), \tag{C-10}$$

where

$$a_n = (Y_0(\lambda_n\rho_0)\, J_0(\lambda_n) - J_0(\lambda_n\rho_0)\, Y_0(\lambda_n)) \sin\frac{\lambda_n}{\mu} \tag{C-11}$$

and

$$b_n = (Y_0(\lambda_n\rho_0)\, J_0(\lambda_n) - J_0(\lambda_n\rho_0)\, Y_0(\lambda_n))^2$$
$$\times\left\{\frac{\alpha}{2\mu^2}\left(1 - \frac{\mu \sin\frac{\lambda_n}{\mu}\cos\frac{\lambda_n}{\mu}}{\lambda_n}\right) + \left(1 - \frac{\beta}{2}\right)\sin^2\frac{\lambda_n}{\mu}\right\} \tag{C-12}$$
$$+\frac{\beta}{2}\sin^2\frac{\lambda_n}{\mu}\left\{\frac{4}{\pi^2\lambda_n^2} - (Y_0(\lambda_n\rho_0)\, J_1(\lambda_n) - J_0(\lambda_n\rho_0)\, Y_1(\lambda_n))^2\right\}.$$

The concentration of the tracer in the aqueous phase is

$$C_0(t) = C_0\, u_1(0, \tfrac{D_a t}{a^2}) = C_0\, u_2(1, \tfrac{D_a t}{a^2}). \tag{C-13}$$

Appendix D

The optimal values of the fitting parameters

Table D-1. The optimal values of the fitting parameters of the homogeneous model for strongly sorbing tracers.

Core	Kd [m^3/kg]	Da [m^2/s]	Kd [m^3/kg]	Da [m^2/s]
^{133}Ba			**^{63}Ni**	
A1	3.0×10^{-3}	1.0×10^{-13}		
A6	2.0×10^{-3}	1.2×10^{-14}	3.7×10^{-3}	1.1×10^{-14}
A8	4.3×10^{-4}	3.0×10^{-14}		
A9	2.0×10^{-3}	3.0×10^{-14}		
A10	8.0×10^{-4}	5.0×10^{-14}		
A12	1.4×10^{-3}	4.0×10^{-14}		
A15	2.1×10^{-3}	5.0×10^{-14}		
A16	1.4×10^{-3}	3.0×10^{-14}		
A17	9.0×10^{-4}	4.0×10^{-14}		
D1	2.0×10^{-3}	2.2×10^{-14}	2.0×10^{-3}	1.4×10^{-14}
D5	1.5×10^{-3}	4.0×10^{-14}		
D6	1.2×10^{-3}	3.0×10^{-14}	1.6×10^{-3}	1.3×10^{-14}
D7	1.5×10^{-3}	7.0×10^{-14}		
D8	8.0×10^{-4}	6.0×10^{-14}		
D12	2.0×10^{-3}	3.0×10^{-14}	2.0×10^{-3}	2.0×10^{-14}
D13	1.5×10^{-3}	7.0×10^{-14}	3.0×10^{-3}	3.0×10^{-14}
D14	8.0×10^{-4}	5.0×10^{-14}		
^{57}Co			**^{226}Ra**	
A8	4.5×10^{-2}	1.0×10^{-14}	6.0×10^{-3}	2.0×10^{-14}
A12			7.0×10^{-3}	3.0×10^{-14}
D7	6.0×10^{-2}	4.0×10^{-14}		
D12	1.0×10^{-1}	1.8×10^{-14}		
D14	1.2×10^{-1}	2.0×10^{-14}		
^{109}Cd				
A6	2.8×10^{-3}	1.8×10^{-14}		

Table D-2. The optimal values of the fitting parameters for ^{137}Cs.

Core	K_d (m^3/kg)	$D_a^{(1)}$ (m^2/s)	$D_a^{(2)}$ (m^2/s)	α
^{137}Cs				
A1	2.5×10^{-2}	6.0×10^{-14}		
A5	6.0×10^{-3}	5.0×10^{-14}		
A6	2.0×10^{-2}	2.0×10^{-14}		
A8	5.0×10^{-4}	1.5×10^{-14}		
A9	1.2×10^{-2}	2.5×10^{-14}	4.0×10^{-12}	0.99996
A10	4.0×10^{-3}	4.0×10^{-14}	4.0×10^{-12}	0.99995
A12	8.0×10^{-3}	3.5×10^{-14}		
A15	1.8×10^{-2}	6.0×10^{-14}		
A16	8.0×10^{-3}	4.0×10^{-14}		
Al7	4.5×10^{-3}	4.0×10^{-14}	4.0×10^{-12}	0.99985
D1	1.2×10^{-2}	2.0×10^{-14}		
D5	8.0×10^{-3}	4.0×10^{-14}		
D6	5.5×10^{-3}	3.5×10^{-14}	6.0×10^{-12}	0.9995
D7	5.0×10^{-3}	9.0×10^{-14}	1.0×10^{-12}	0.9998
D8	5.0×10^{-3}	5.0×10^{-14}		
D12	1.1×10^{-2}	4.0×10^{-14}	1.5×10^{-12}	0.9999
D13	6.0×10^{-3}	7.0×10^{-14}	7.0×10^{-12}	0.99982
D14	4.2×10^{-3}	4.3×10^{-14}	7.0×10^{-12}	0.99996

Table D-3. The optimal values of the fitting parameters for ^{22}Na.

Core	K_d (m^3/kg)	$D_a^{(1)}$ [m^2/s]	$D_a^{(2)}$ [m^2/s]	α
^{22}Na				
A1	1.4×10^{-5}	5.0×10^{-13}	4.0×10^{-12}	0.6
A5	1.1×10^{-5}	6.0×10^{-14}	4.0×10^{-12}	0.83
A6	4.9×10^{-5}	2.0×10^{-14}	2.0×10^{-12}	0.83
A8	4.0×10^{-4}	3.0×10^{-14}	5.0×10^{-12}	0.994
A9	1.4×10^{-5}	8.0×10^{-14}	3.0×10^{-12}	0.8
A10	6.9×10^{-6}	5.0×10^{-14}	3.3×10^{-12}	0.59
A12	1.0×10^{-5}	3.0×10^{-14}	2.0×10^{-12}	0.78
A15	3.3×10^{-5}	3.0×10^{-14}	3.0×10^{-12}	0.92
A16	3.3×10^{-5}	3.0×10^{-14}	3.0×10^{-12}	0.93
A17	1.8×10^{-6}	3.0×10^{-14}	5.0×10^{-12}	0.77
D1	3.3×10^{-5}	1.0×10^{-13}	1.8×10^{-12}	0.64
D5	4.4×10^{-5}	5.0×10^{-14}	2.2×10^{-12}	0.75
D6	1.7×10^{-5}	2.0×10^{-13}	3.0×10^{-12}	0.6
D7	1.6×10^{-5}	3.0×10^{-12}		
D8	3.9×10^{-5}	4.0×10^{-14}	1.7×10^{-12}	0.69
D12	1.6×10^{-5}	5.0×10^{-14}	4.2×10^{-12}	0.4
D13	1.8×10^{-5}	5.0×10^{-14}	4.0×10^{-12}	0.35
D14	1.4×10^{-5}	2.7×10^{-12}		

Table D-4. The optimal values of the fitting parameters for ^{36}Cl.

Core	ϵ [%]	$D_a^{(1)}$ [m^2/s]	$D_a^{(2)}$ [m^2/s]	α
^{36}Cl				
A6	0.133	7.0×10^{-14}	6.0×10^{-12}	0.88
A9	0.136	4.0×10^{-14}	6.0×10^{-12}	0.93
A12	0.134	3.0×10^{-14}	5.0×10^{-12}	0.94
A16	0.133	6.0×10^{-14}	9.0×10^{-12}	0.96
A17	0.129	5.0×10^{-14}	9.0×10^{-12}	0.89
D1	0.109	5.0×10^{-14}	4.3×10^{-12}	0.78
D14	0.123	4.0×10^{-14}	9.0×10^{-12}	0.89

Appendix E

Fitting figures for the penetration profiles

^{133}Ba

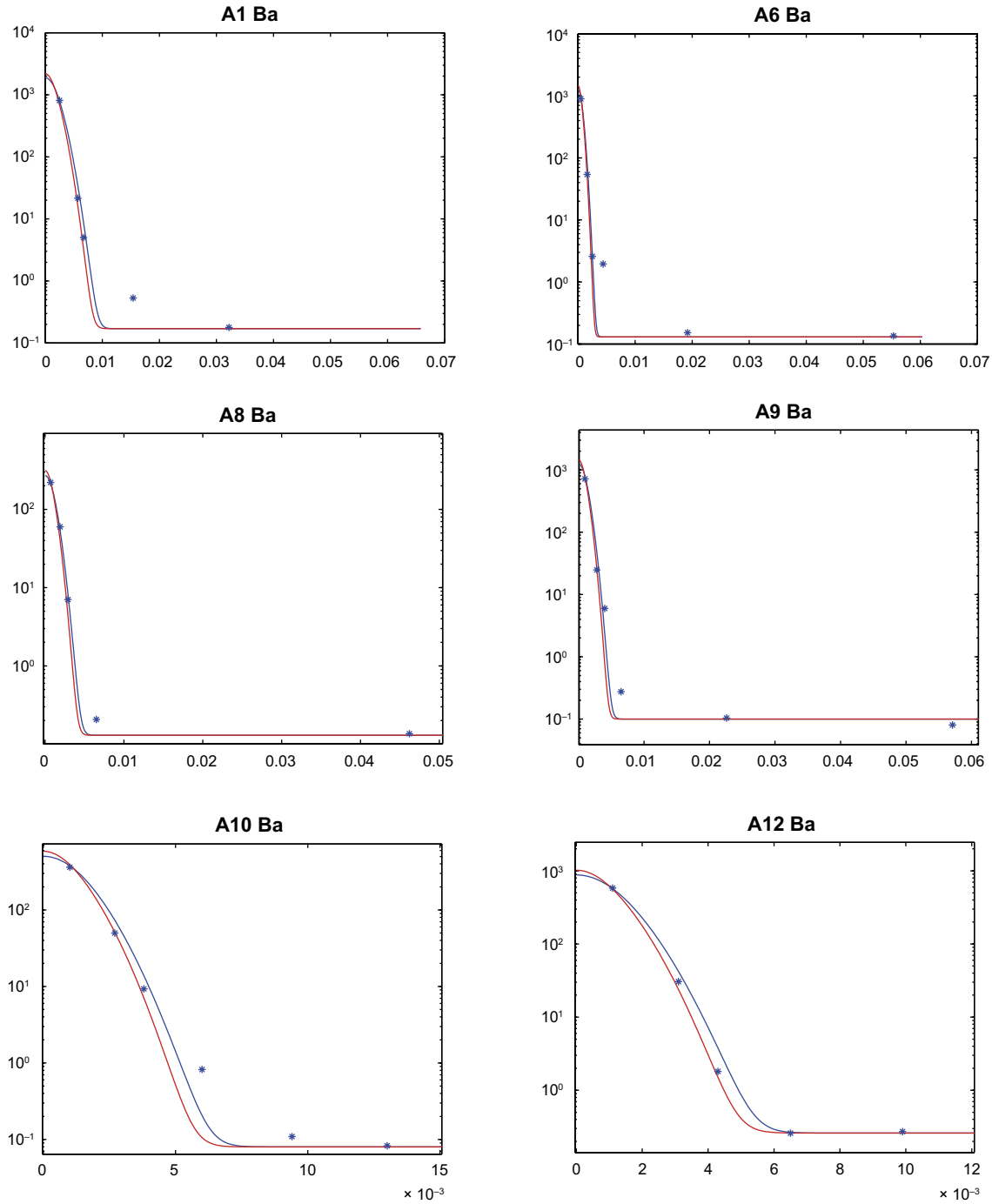

Figure E-1. *The concentration of ^{133}Ba [Bq/g] vs distance [m] for A and D cores.*

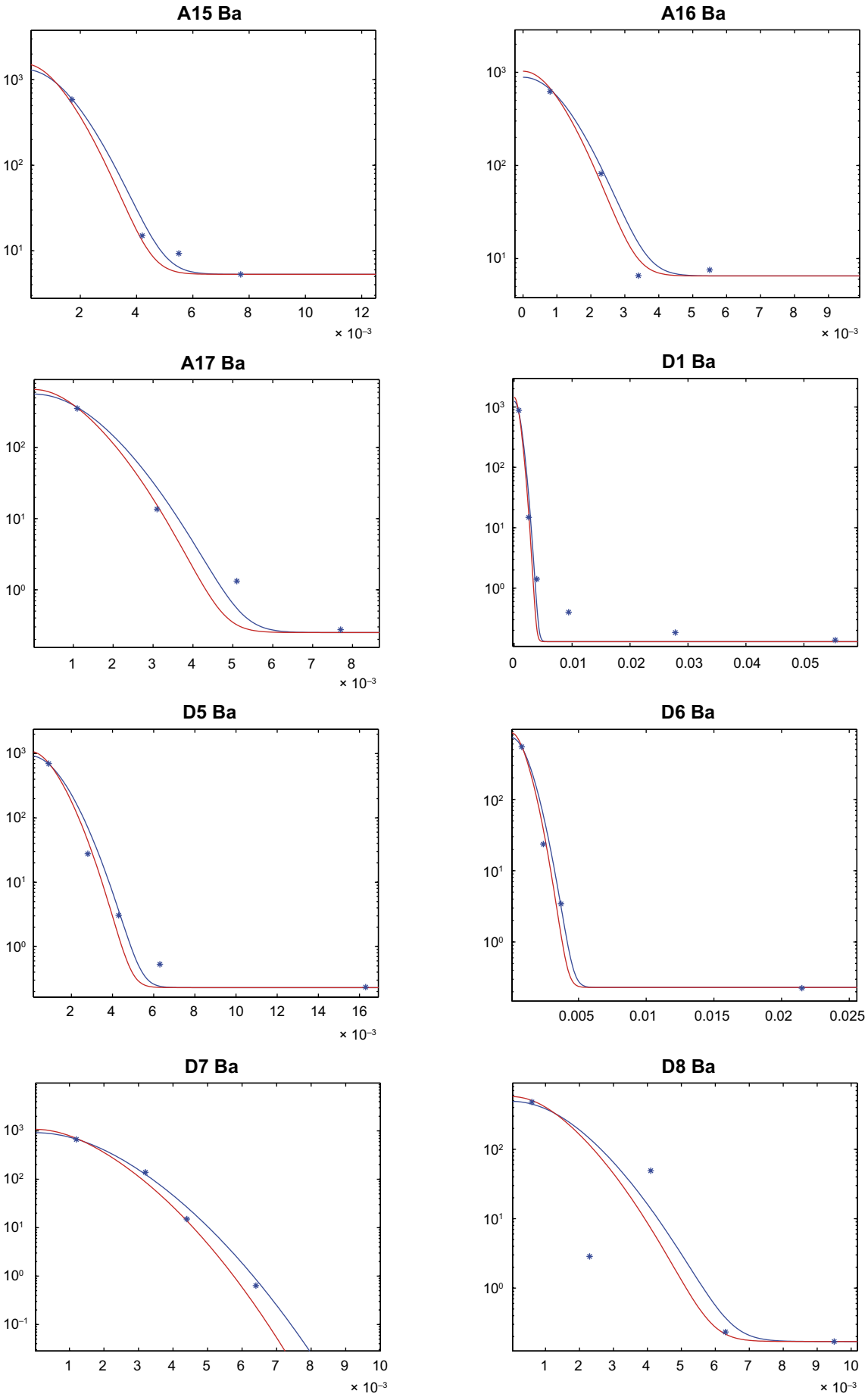

Figure E-1. *Continued.*

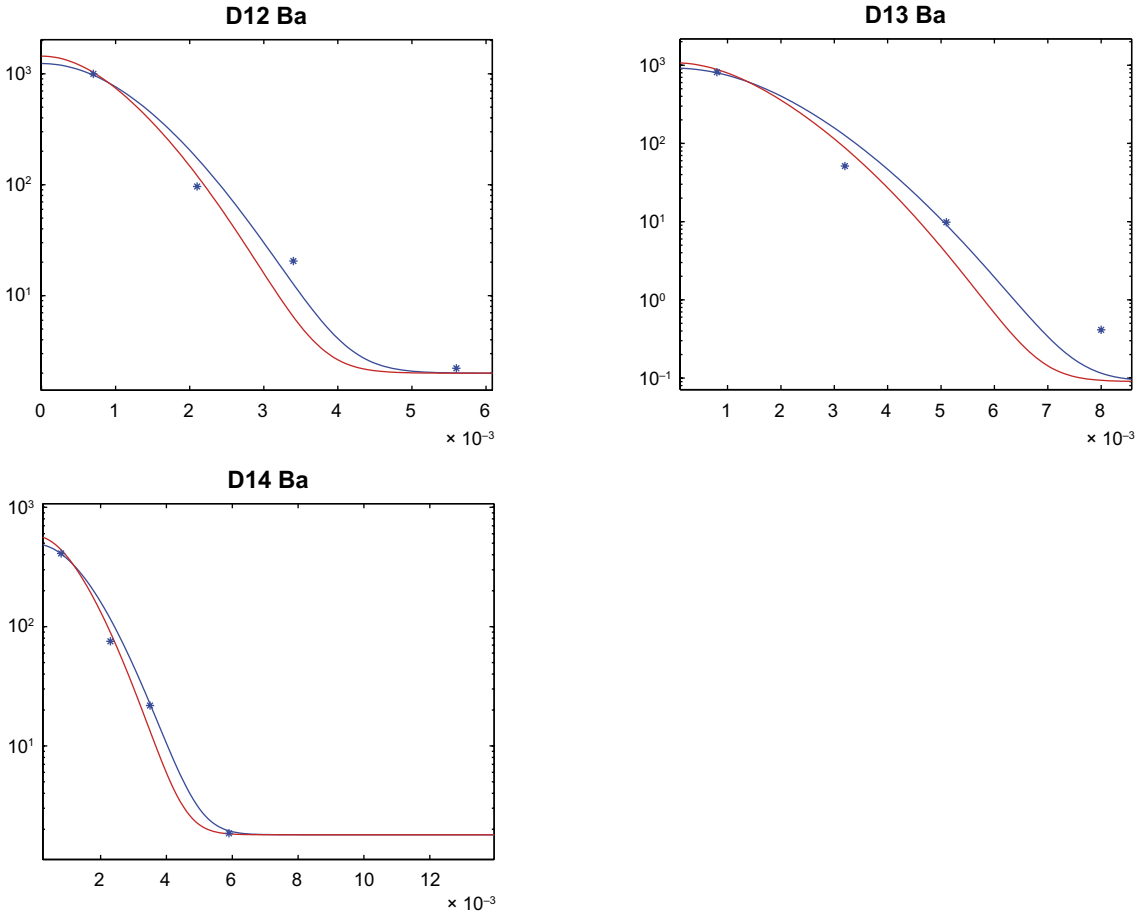

Figure E-1. *Continued.*

^{137}Cs

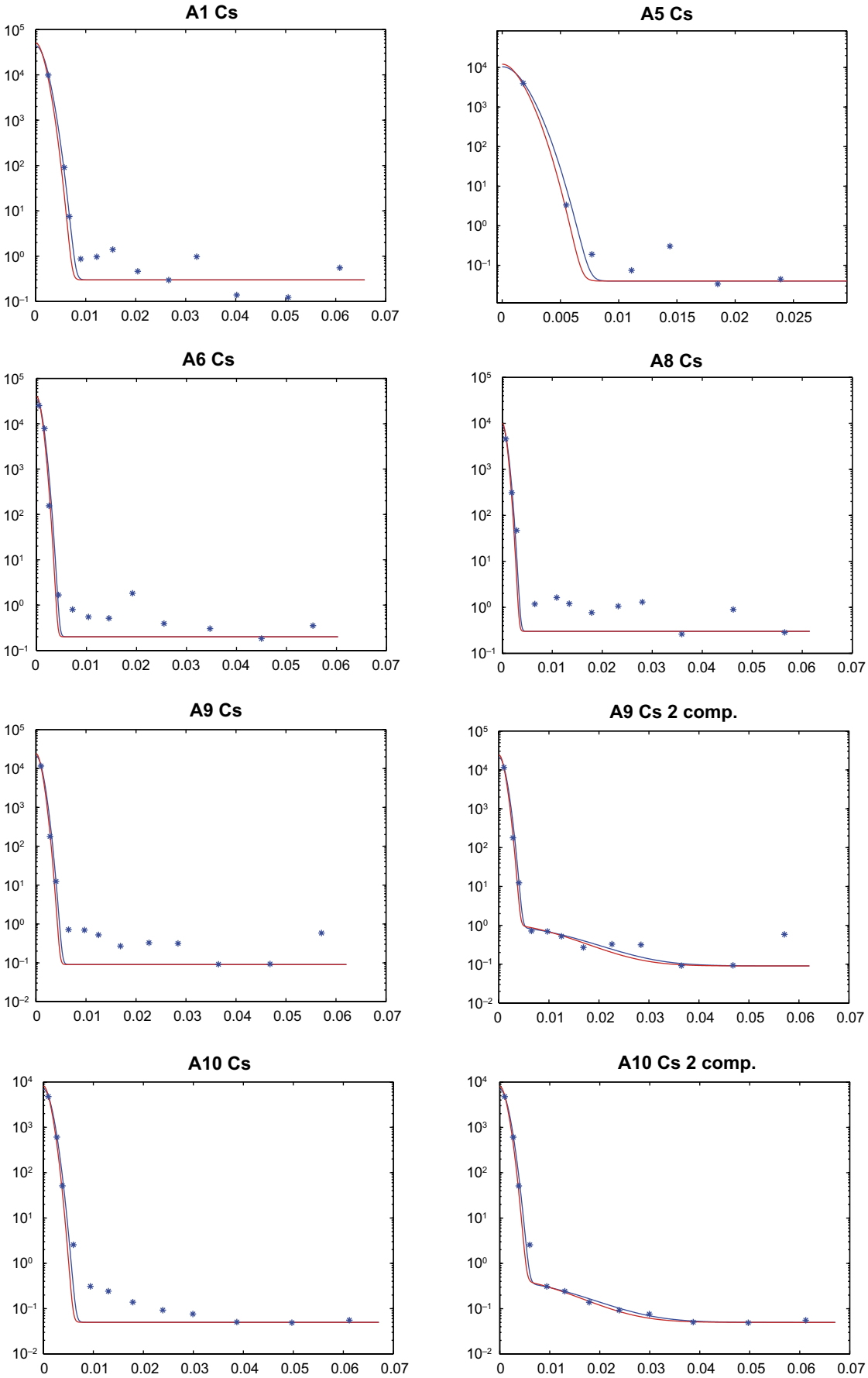

Figure E-2. *The concentration of ^{137}Cs [Bq/g] vs distance [m] for A and D cores.*

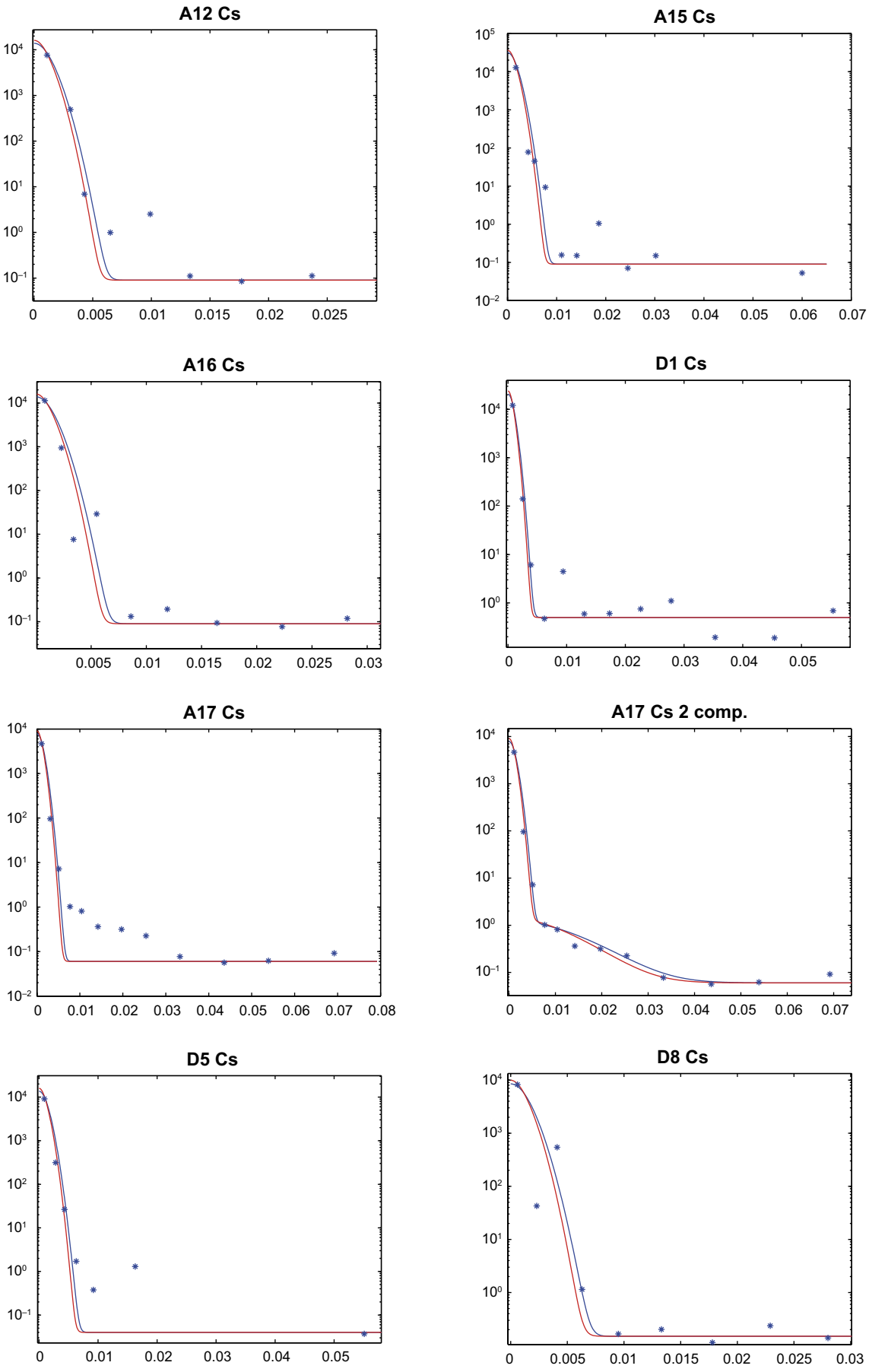

Figure E-2. *Continued.*

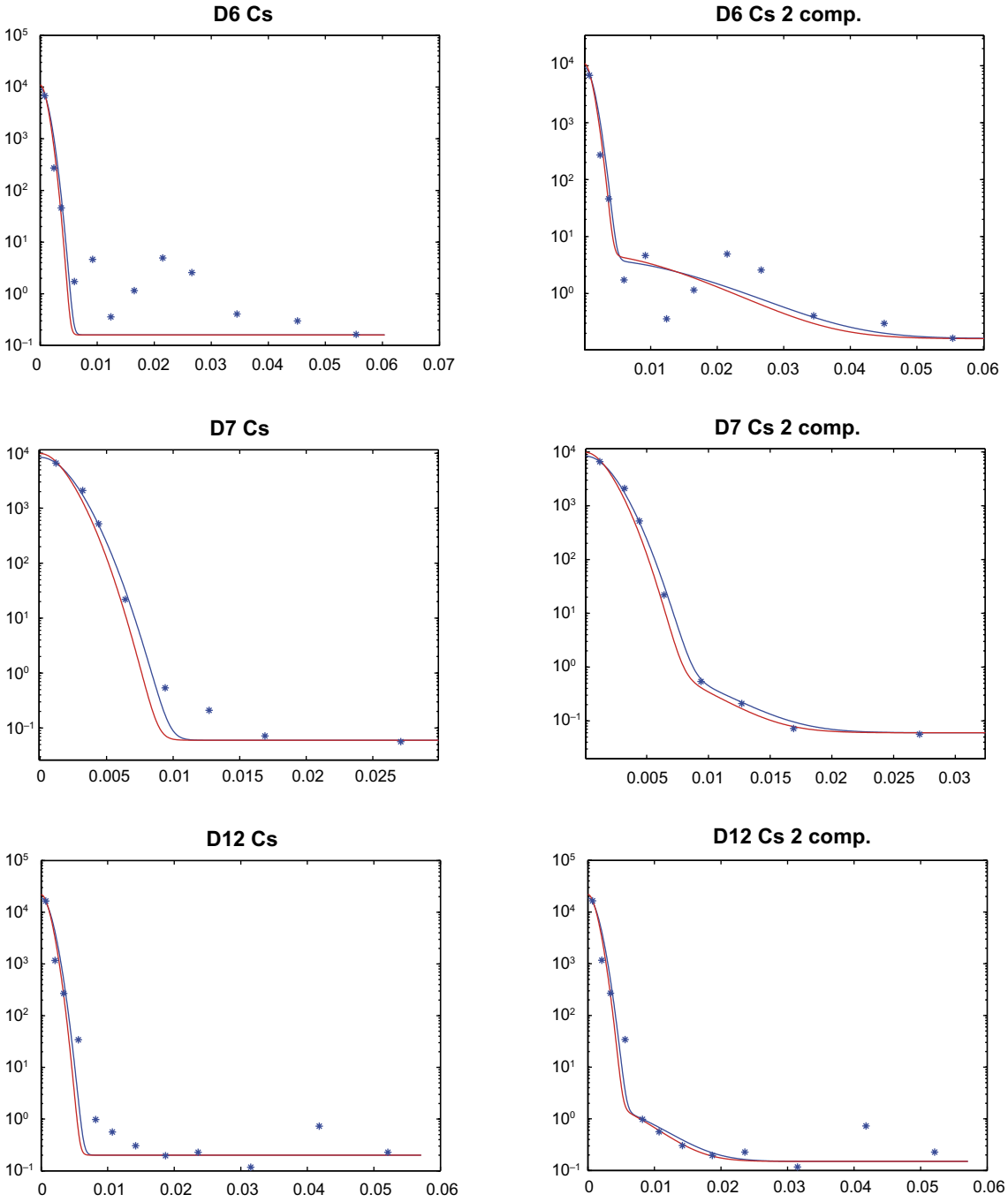

Figure E-2. *Continued.*

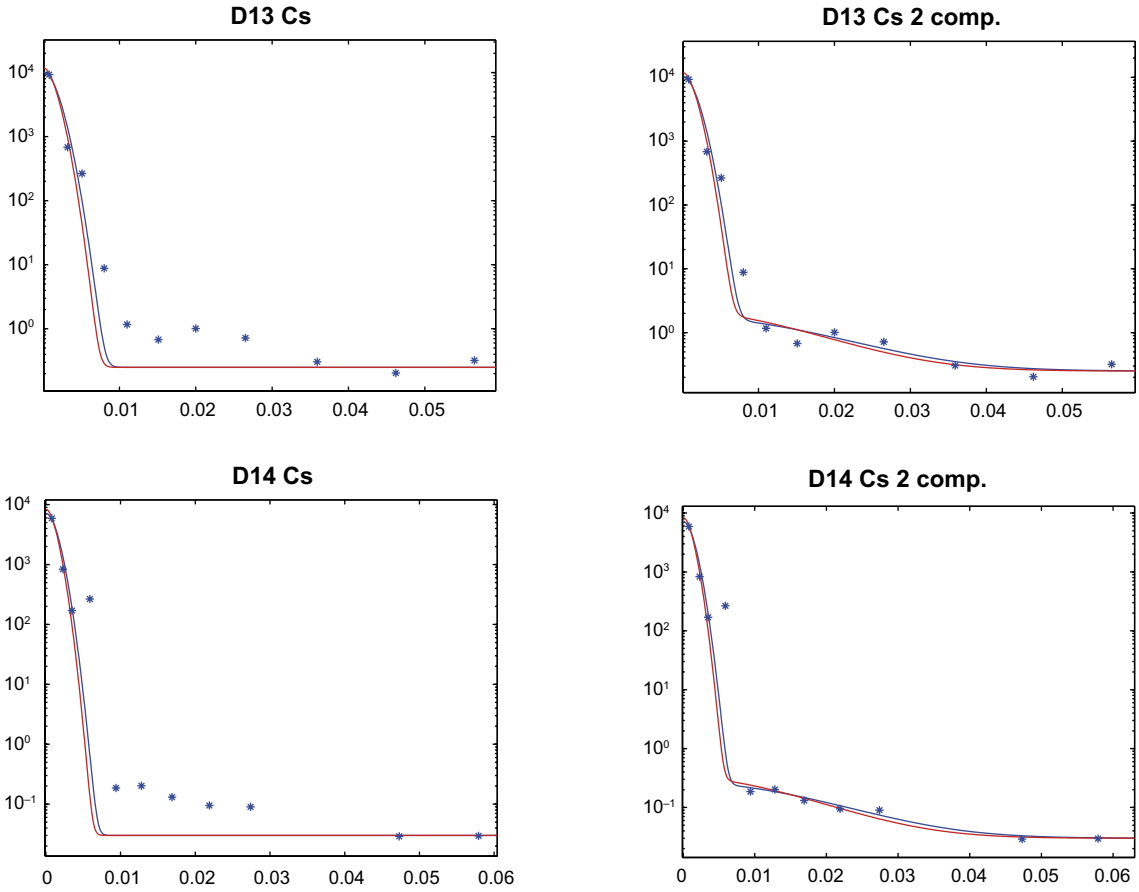

Figure E-2. *Continued.*

^{22}Na

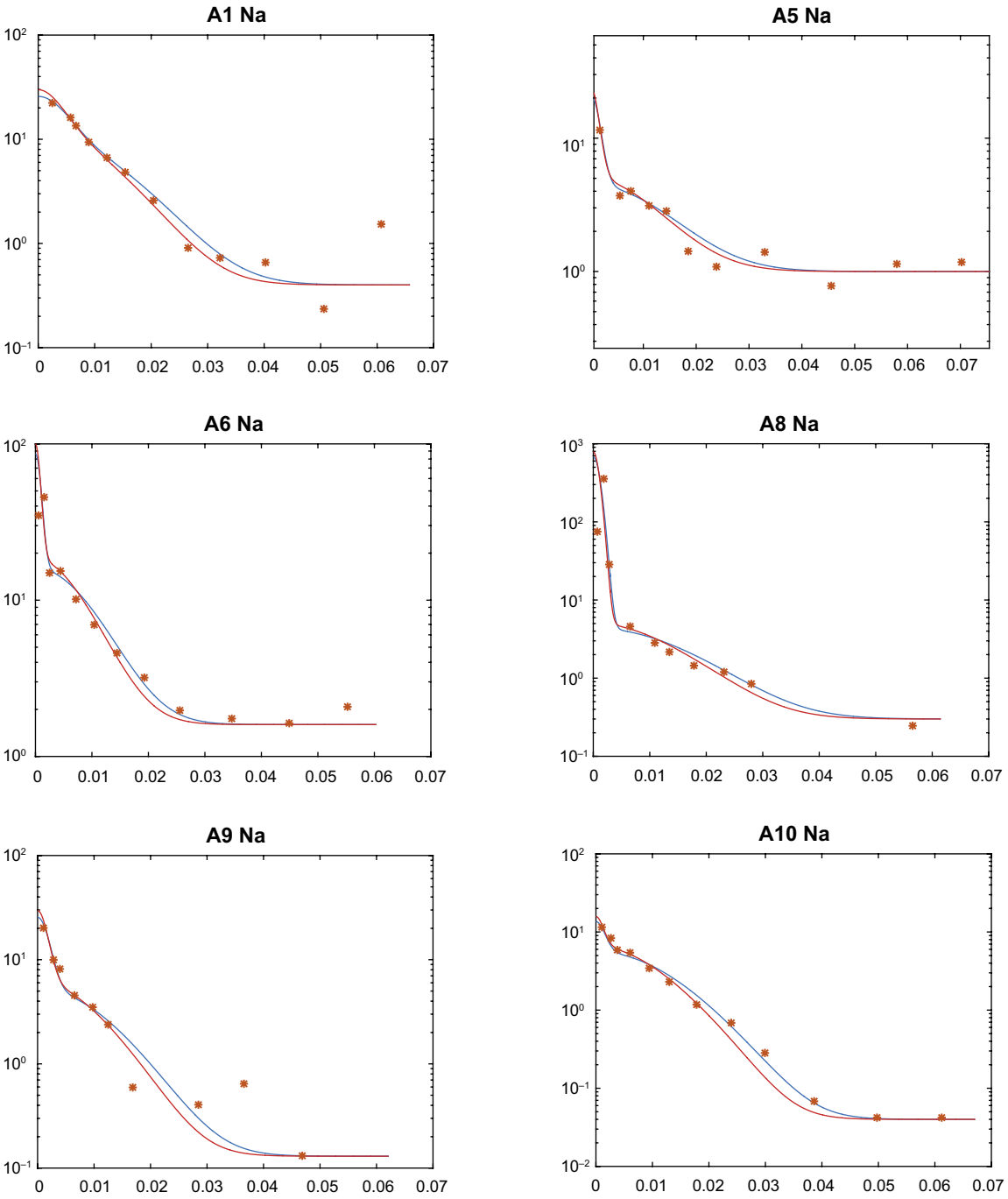

Figure E-3. *The concentration of ^{22}Na [Bq/g] vs distance [m] for A and D cores.*

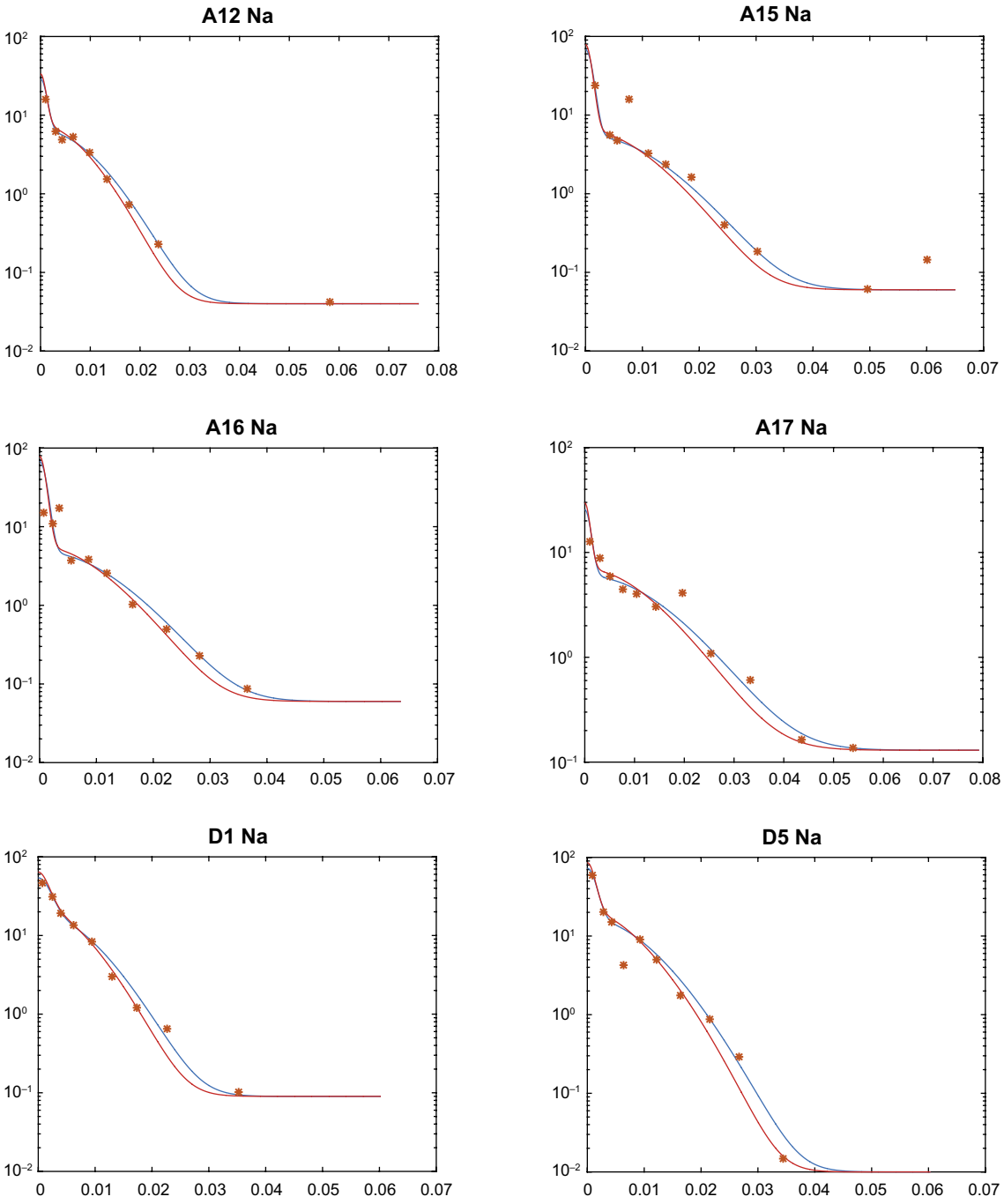

Figure E-3. *Continued.*

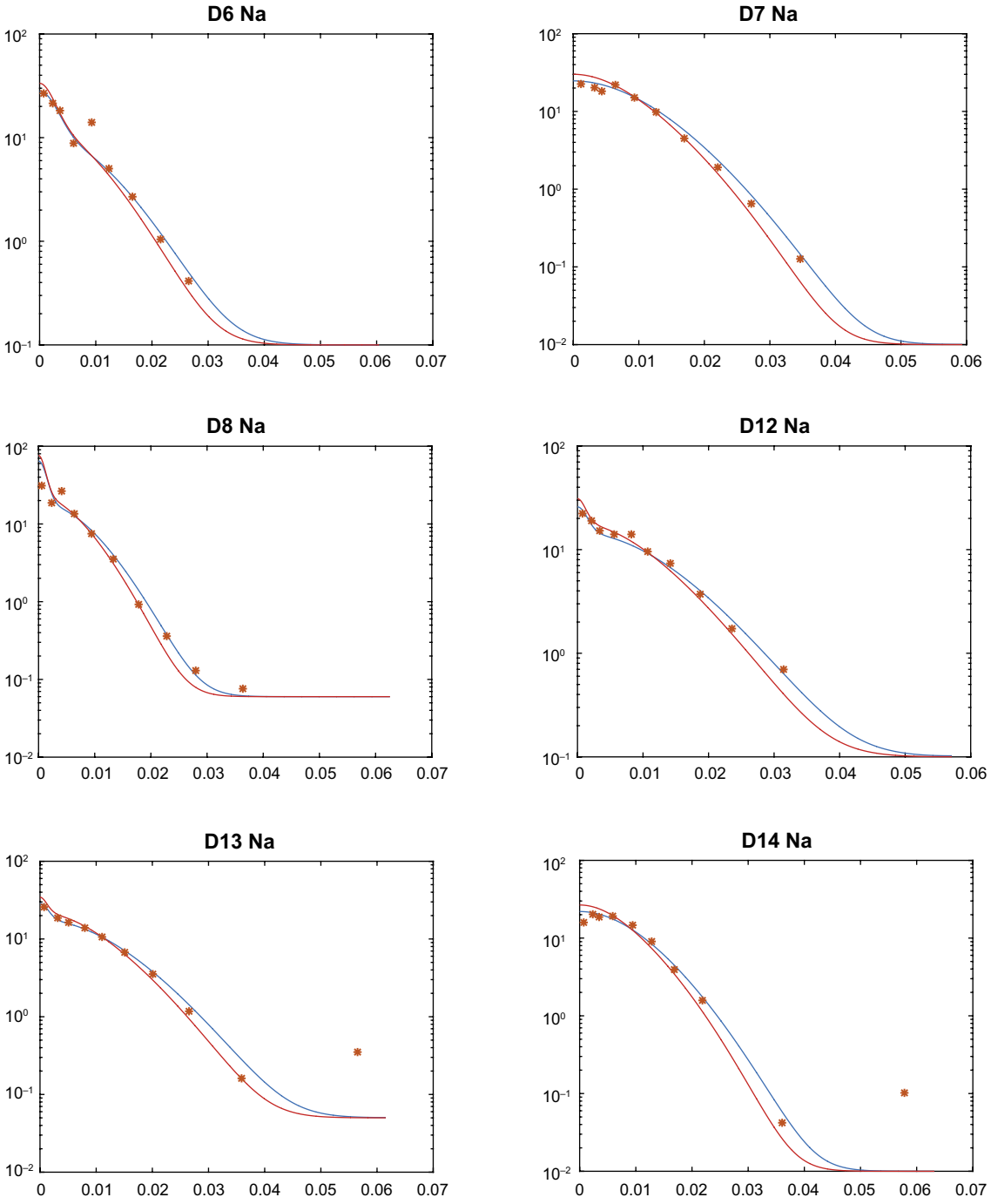

Figure E-3. *Continued.*

^{36}Cl

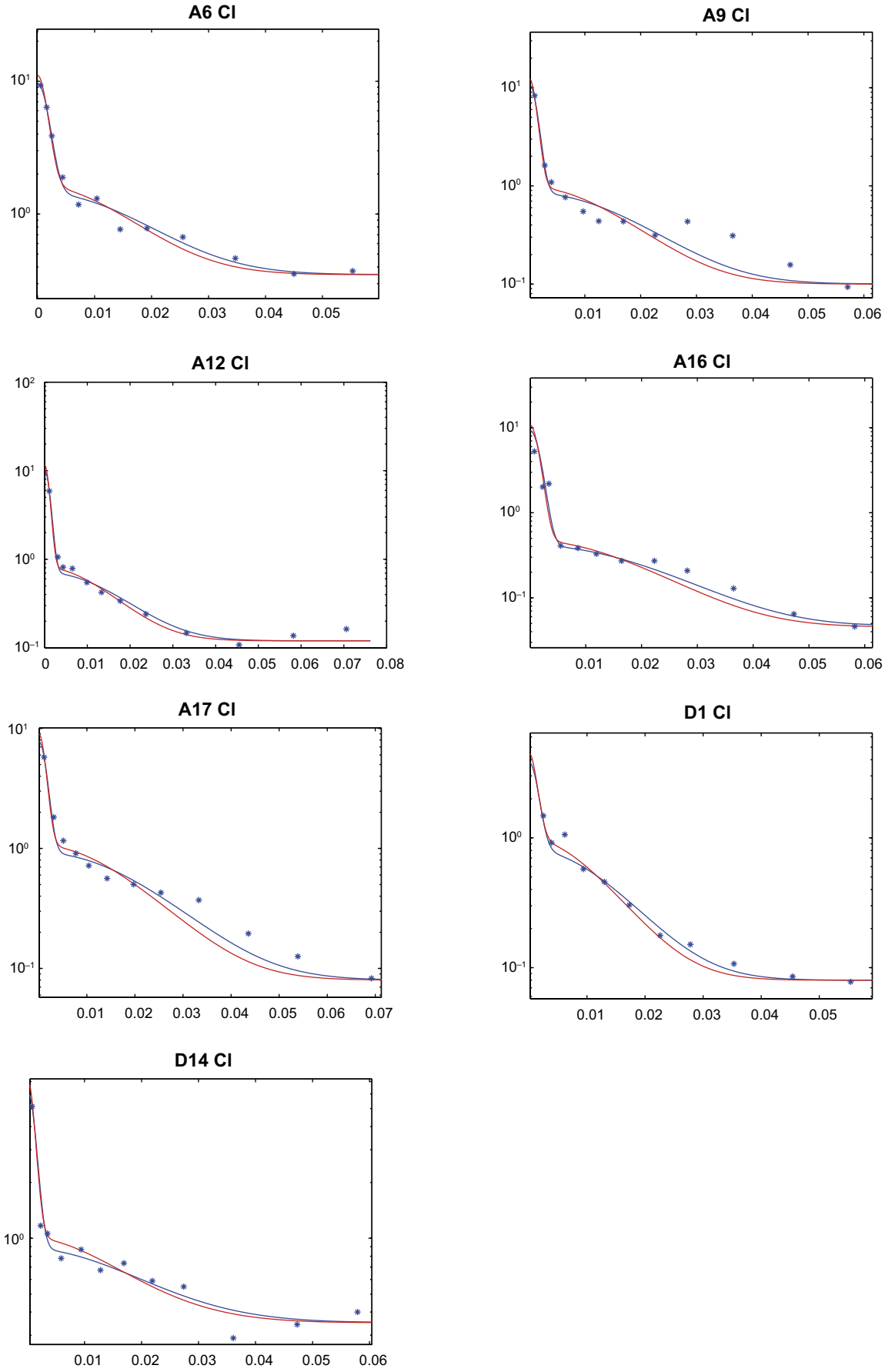

Figure E-4. *The concentration of ^{36}Cl [Bq/g] vs distance [m] for A and D cores.*

^{57}Co

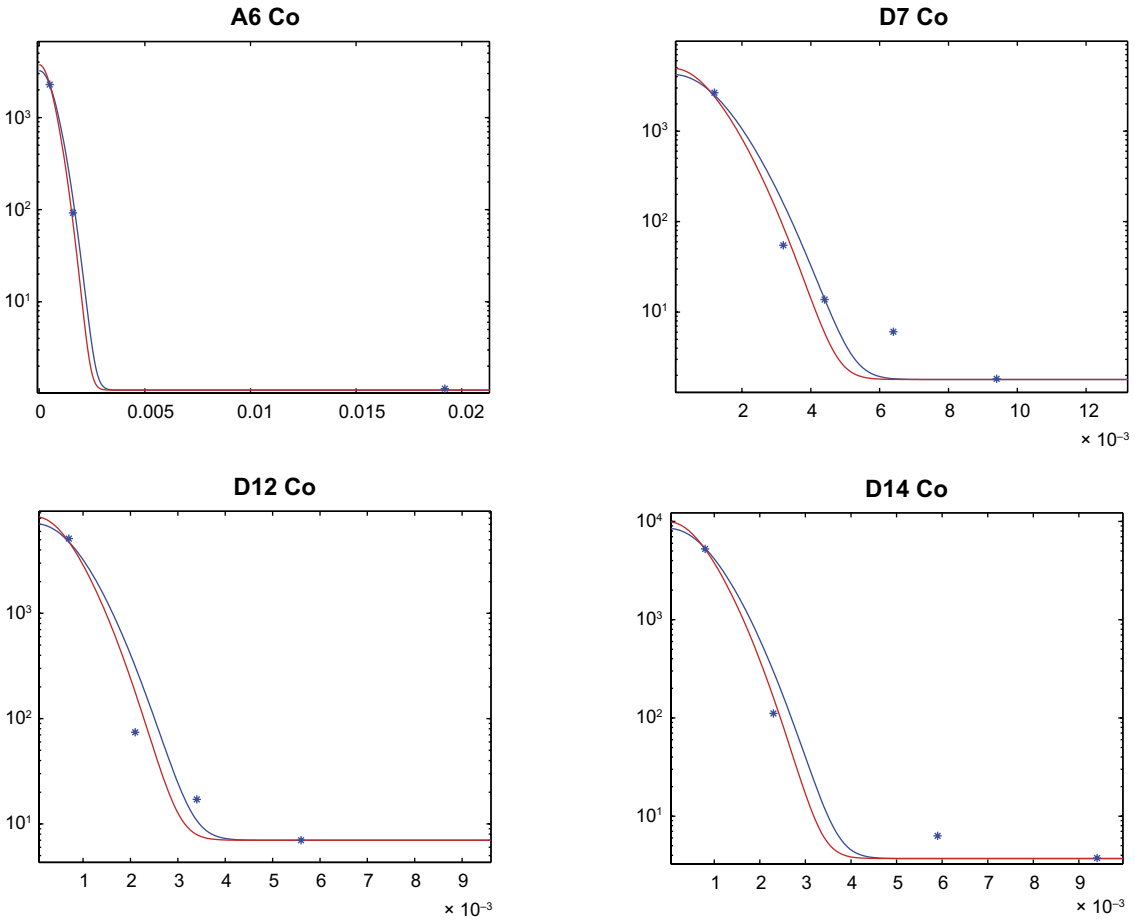

Figure E-5. *The concentration of ^{57}Co [Bq/g] vs distance [m] for A and D cores.*

^{226}Ra

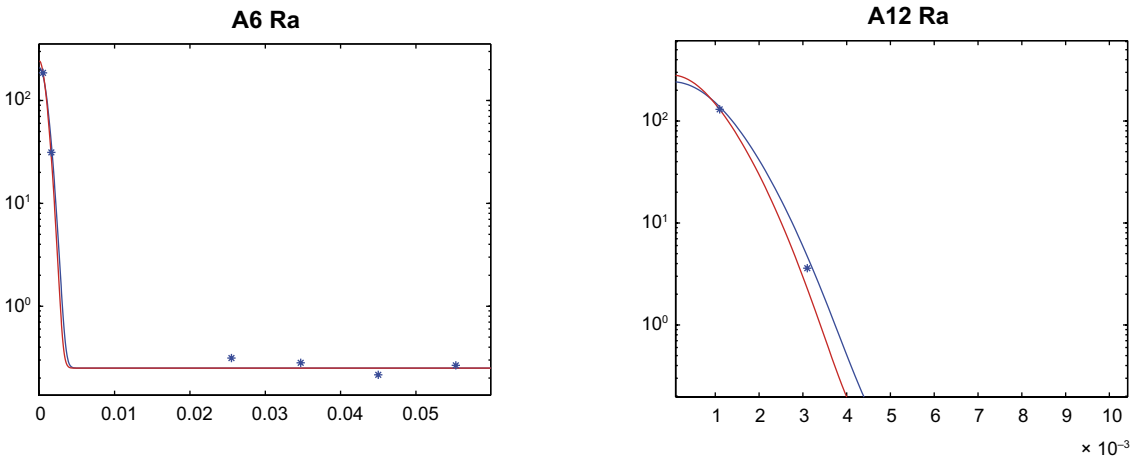

Figure E-6. *The concentration of ^{226}Ra [Bq/g] vs distance [m] for A cores.*

^{63}Ni and ^{109}Cd

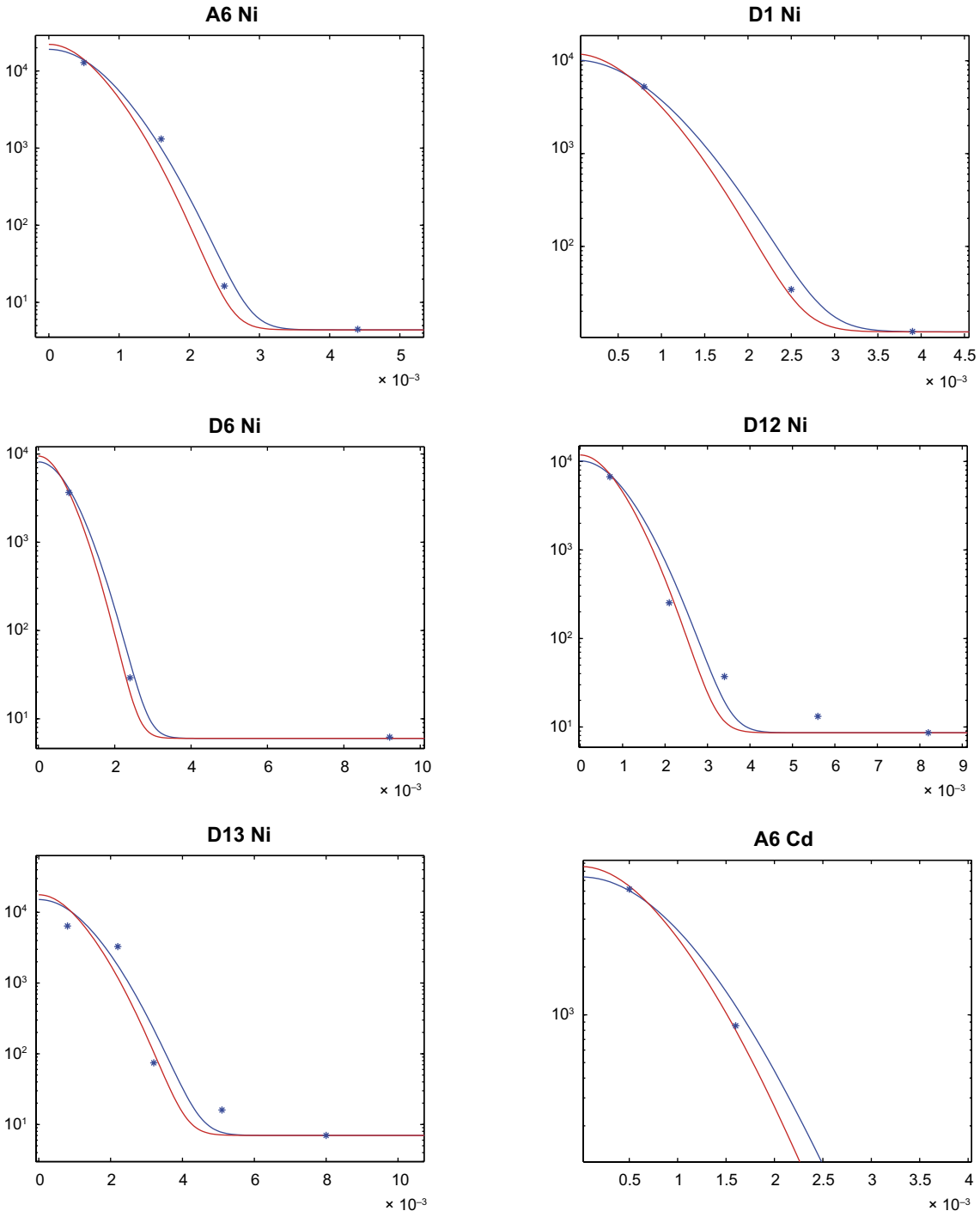

Figure E-7. *The concentration of ^{63}Ni and ^{109}Cd [Bq/g] vs distance [m] for A and D cores.*

Appendix F

Plots of the aqueous phase model

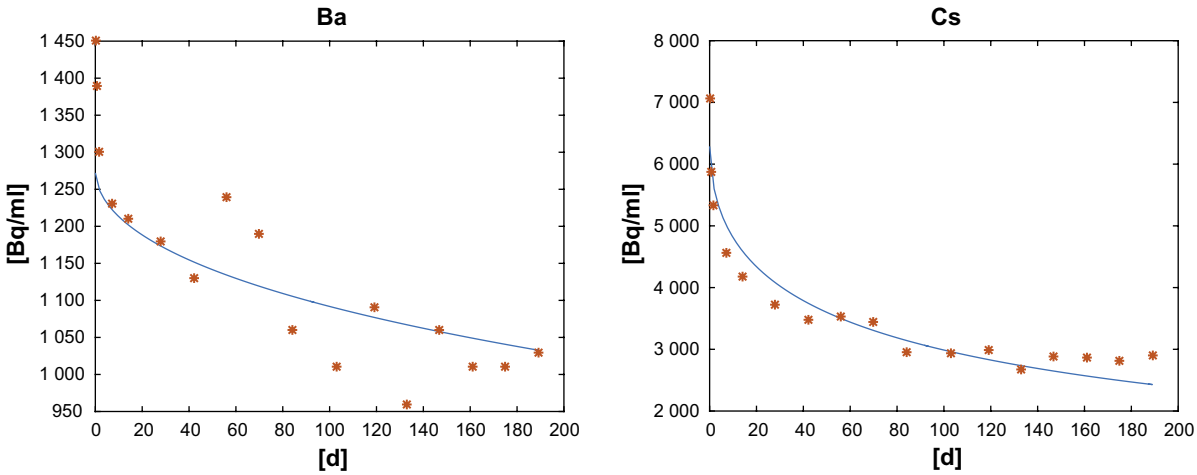

Figure F-1. *The concentration of ^{133}Ba and ^{137}Cs tracers in the aqueous phase of the solution reservoir.*

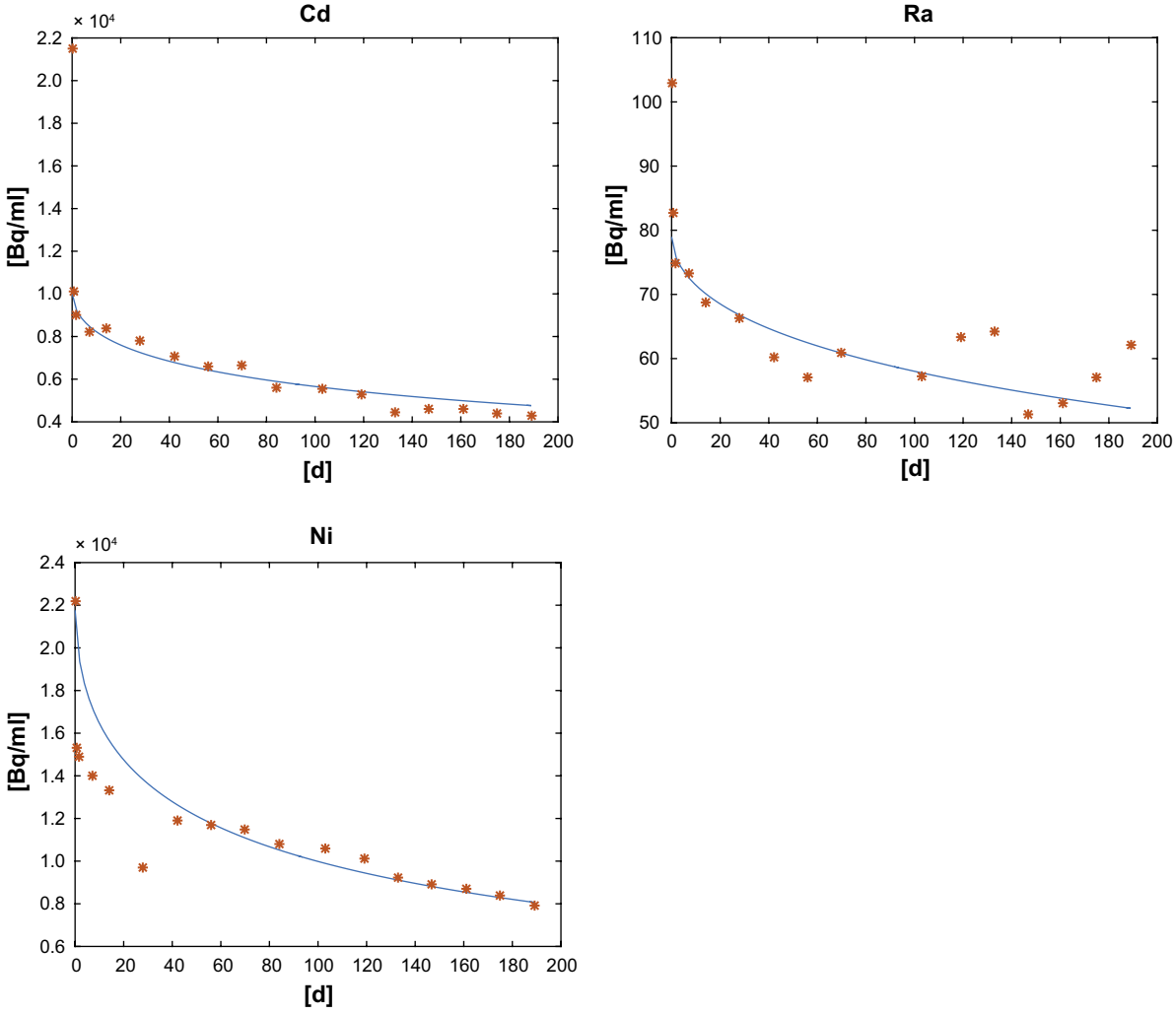

Figure F-2. *The concentration of ^{63}Ni, ^{109}Cd and ^{226}Ra tracers in the aqueous phase of the solution reservoir.*

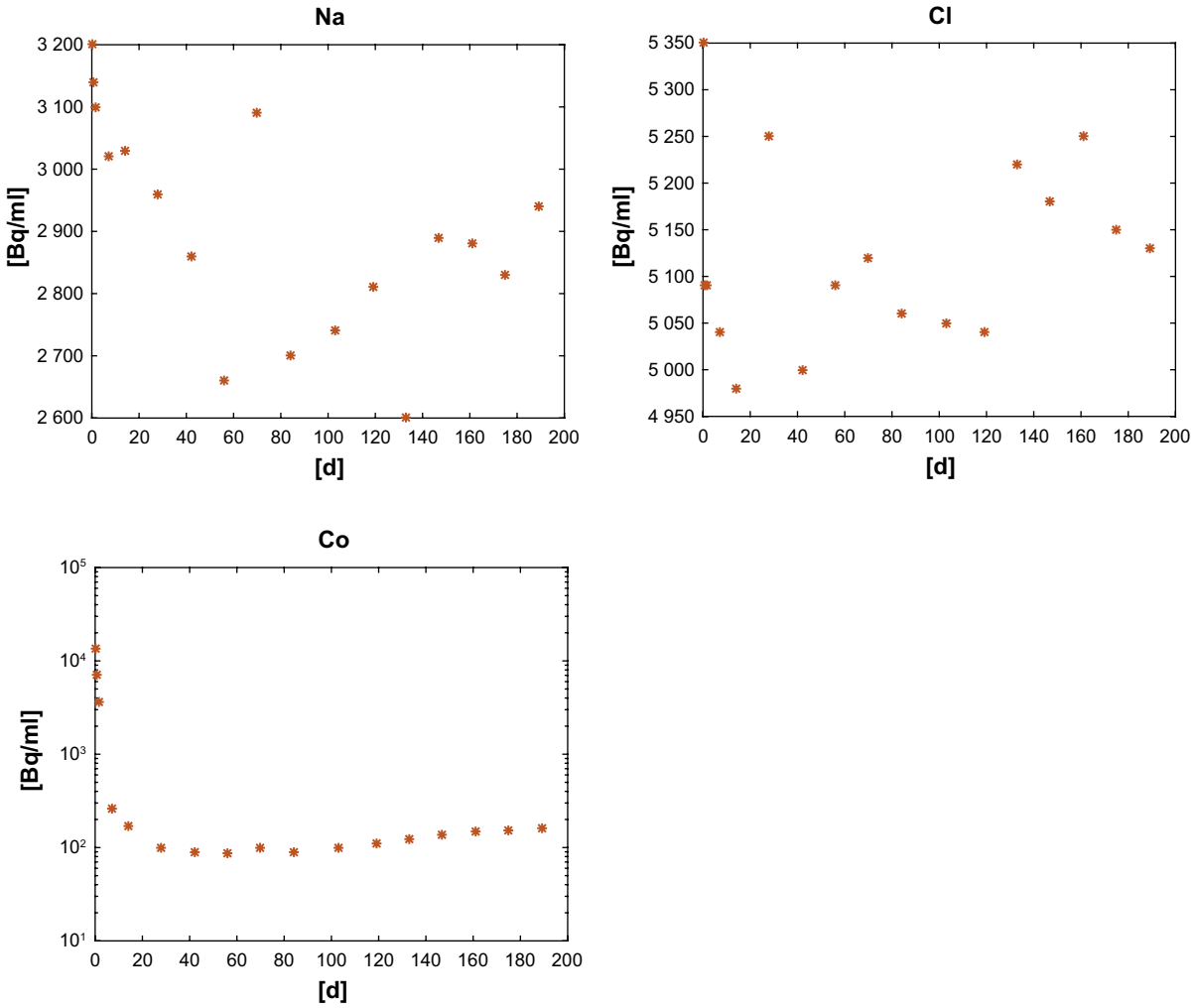

Figure F-3. *The concentration of ^{22}Na, ^{36}Cl and ^{57}Co tracers in the aqueous phase of the solution reservoir.*

Arkitektkopia AB, Bromma, 2021

SKB is responsible for managing spent nuclear fuel and radioactive waste produced by the Swedish nuclear power plants such that man and the environment are protected in the near and distant future.

skb.se